

Photoinduced Electron-Transfer Kinetics of Singly Labeled Ruthenium Bis(bipyridine) Dicarboxybipyridine Cytochrome *c* Derivatives[†]

Bill Durham,* Lian Ping Pan, Joan E. Long, and Francis Millett

Department of Chemistry and Biochemistry, University of Arkansas, Fayetteville, Arkansas 72701

Received March 24, 1989; Revised Manuscript Received June 22, 1989

ABSTRACT: Cytochrome *c* derivatives labeled at specific lysine amino groups with ruthenium bis(bipyridine) dicarboxybipyridine [Ru^{II}(bpy)₂(dcbpy)] were prepared by using the procedure described previously [Pan, L. P., Durham, B., Wolinska, J., & Millett, F. (1988) *Biochemistry* 27, 7180-7184]. Four additional singly labeled derivatives were purified, bringing the total number to 10. These derivatives have a strong luminescence emission centered at 662 nm arising from the excited state, Ru^{II}*. Transient absorption spectroscopy was used to directly measure the rate constants for the photoinduced electron-transfer reaction from Ru^{II}* to the ferric heme group (*k*₁) and for the thermal back-reaction from the ferrous heme group to Ru^{III} (*k*₂). The rate constants were found to be *k*₁ = 14 × 10⁶ s⁻¹ and *k*₂ = 24 × 10⁶ s⁻¹ for the derivative modified at lysine 72, which has a distance of 8-16 Å between the ruthenium and heme groups. Similar rate constants were found for the derivatives modified at lysines 13 and 27, which have distances of 6-12 Å separating the ruthenium and heme groups. The rate constants were significantly slower for the derivatives modified at lysine 25 (*k*₁ = 1 × 10⁶ s⁻¹, *k*₂ = 1.5 × 10⁶ s⁻¹) and lysine 7 (*k*₁ = 0.3 × 10⁶ s⁻¹, *k*₂ = 0.5 × 10⁶ s⁻¹), which have distances of 9-16 Å. Transients due to photoinduced electron transfer could not be detected for the remaining derivatives, which have larger distances between the ruthenium and heme groups. The large electron-transfer rate constants observed for these derivatives are consistent with the large driving force of the reaction and the low reorganization energy of the Ru(bpy)₂(dcbpy) complex.

The factors involved in long-range biological electron-transfer reactions have been studied by using a wide range of different approaches. Winkler et al. (1982) and Isied et al. (1982) introduced the use of tethered ruthenium complexes by specifically attaching a Ru^{II}(NH₃)₅ group to histidine 33 of cytochrome *c*. Intramolecular electron transfer from Ru^{II} to the ferric heme was found to occur with a rate constant of 30-55 s⁻¹. This reaction has a driving force of 0.11 eV and a separation of about 12 Å between the ruthenium and heme groups. Rather surprisingly, Bectold et al. (1986) found that the rate of electron transfer from the ferrous heme group of cytochrome *c* to Ru^{III}(NH₃)₄(isonicotinamide)-histidine 33 was over 10⁵ times slower than the above rate, even though the driving force was larger (0.18 eV). This result suggested that the specific protein structure between the donor and acceptor groups might play an important role in electron transfer. Elias et al. (1988) recently explored the dependence of electron transfer on driving force using a zinc-substituted derivative of Ru^{III}(NH₃)₂-histidine 33 cytochrome *c*. The zinc porphyrin has a long-lived excited state that provides a large driving force (0.88 eV) for electron transfer to the ruthenium group. The rate constants for the photoinduced reaction and the thermal back-reaction were found to be 7.7 × 10⁵ s⁻¹ and 1.6 × 10⁶ s⁻¹, respectively. These results were consistent with a reorganization energy of about 1.5 eV using the semiclassical theory introduced by Marcus. Axup et al. (1988) have recently studied electron transfer in a series of zinc-substituted myoglobin derivatives labeled at different histidine residues with Ru^{III}(NH₃)₅. The distance dependence of electron transfer could be described by an exponential decrease with distance scaled by a "β" factor of 0.9-1.0 Å⁻¹. Intramolecular electron-transfer studies have also been carried out on ruthenium-labeled azurin, plastocyanin, and myoglobin derivatives (Kostič et al., 1983;

Crutchley et al., 1986; Jackman et al., 1988; Axup et al., 1988), mixed-metal hybrid hemoglobins (McGourty et al., 1987), and organic redox agents coupled by spacers (Closs et al., 1986).

We have recently introduced a new class of cytochrome *c* derivatives that are singly labeled at individual lysine amino groups with ruthenium bis(bipyridine) dicarboxybipyridine [Ru^{II}(bpy)₂(dcbpy)]¹ (Pan et al., 1988). The purification of four additional Ru^{II}(bpy)₂(dcbpy)-cytochrome *c* derivatives is described in the present paper, bringing the total number to ten. These derivatives have a strong luminescence emission centered at 662 nm assigned to the excited state, Ru^{II}*. Pan et al. (1988) reported that the luminescence decay rates were inversely related to the distances between the ruthenium groups and the heme group, suggesting the possibility of electron-transfer and/or energy-transfer quenching mechanisms. In the present paper, we report on the use of transient absorption spectroscopy to directly measure the rate constants for the photoinduced electron-transfer reaction from Ru^{II}* to the ferric heme group and for the thermal back-reaction from the ferrous heme group to Ru^{III}.

EXPERIMENTAL PROCEDURES

Materials. Horse heart cytochrome *c* was obtained from Sigma Chemical Co. (type VI), and 4,4'-dimethyl-2,2'-bipyridine was obtained from GFS Chemicals. *N*-Hydroxy-succinimide and dicyclohexylcarbodiimide were obtained from Pierce Chemical Co. 4,4'-Dicarboxybipyridine (dcbpy) was prepared from 4,4'-dimethylbipyridine by the method of Sprintschnik et al., (1978). Ru^{II}(bpy)₂(CO₃) was prepared as described by Johnson et al. (1978). The mono *N*-

[†] This work was supported by NIH Grants GM20488 and RR07101.

¹ Abbreviations: bpy, 2,2'-bipyridine; dcbpy, 4,4'-dicarboxy-2,2'-bipyridine.

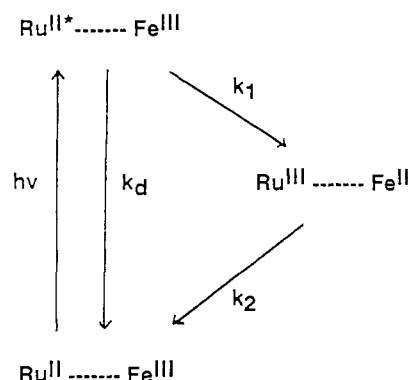
hydroxysuccinimide ester of dcbpy was prepared as described by Pan et al. (1988).

Preparation of $Ru^{II}(bpy)_2(dcbpy)$ -Cytochrome *c* Derivatives. Horse heart cytochrome *c* (20 mM in 2 mL of 50 mM Tris-HCl, pH 8.0) was mixed with freshly prepared mono *N*-hydroxysuccinimide ester of dcbpy (80 mM in 2 mL of 50 mM Tris-HCl, pH 8.0) and incubated for 2 h at 25 °C as described by Pan et al. (1988). The sample was chromatographed on a 2.5 × 70 cm Bio-Rex 70 column using an exponential gradient from 50 mM ammonium phosphate, pH 7.2, to 160 mM ammonium phosphate, pH 7.2. Each of fractions 1–7 was concentrated on a small Bio-Rex 70 column and rechromatographed on a 1.5 × 25 cm column of Whatman sulfopropyl SE-53 using an exponential gradient from 20 to 250 mM sodium phosphate, pH 6.0. Each of the purified dcbpy-cytochrome *c* fractions was concentrated to 1 mM and treated with 10 mM $Ru^{II}(bpy)_2CO_3$ in 100 mM sodium acetate, pH 4.0, for 24 h at 25 °C in the dark. The sample was passed through a small Bio-Gel P-2 column to remove excess reagent and then chromatographed on a 0.6 × 45 cm Whatman CM-32 column using a gradient from 20 to 400 mM sodium phosphate, pH 6.0. UV/visible spectra were recorded on a Hewlett-Packard 8452 diode array spectrophotometer. The redox potential of the heme group in the cytochrome *c* derivatives was determined by titration with ferricyanide, as described by Smith et al. (1977).

Identification of the Lysine Modified in the $Ru(bpy)_2(dcbpy)$ -Cytochrome *c* Derivatives. Each derivative was dialyzed into 0.1 M Bicine, pH 8.0, at a concentration of 1 μg/μL, and digested with 50 ng/μL TPCCK-treated trypsin for 15 h at 37 °C. The tryptic digests were separated on a Dynamax 300-Å reverse-phase HPLC column using a linear gradient from 0.01% trifluoroacetic acid to 100% methanol. The gradient was generated on a Spectra Physics SP 8700 solvent delivery system, and the eluent was monitored at 210 and 294 nm on Kratos 757 and Tracor 980A detectors in series. The HPLC chromatogram of each purified fraction 3B, 4A, 4B, and 4' contained a single ruthenium-labeled peptide which absorbed at 294 nm. The specific lysine labeled by ruthenium was determined by amino acid analysis as described by Pan et al. (1988).

Transient Absorption Kinetics. Transient absorbance measurements were carried out by laser flash photolysis of anaerobic solutions containing 5–20 μM derivative in 100 mM sodium phosphate, pH 7.0, at 25 °C. The excitation pulse was obtained from a Quanta Ray dye laser (coumarin 460 at 460 nm) pumped by the third harmonic of a Nd:YAG laser. A pulsed 75-W xenon arc lamp was used as the probe source. The optical axes of the probe and excitation beams formed an angle of 9°. A shutter and appropriate cutoff filters were used to minimize the impact of the probe beam on the sample. After passing through the sample, the probe beam passed through an appropriate cutoff filter, entered a monochromator (Schoeffel GM-252), and was detected by an R446 PMT. A five-dynode configuration (Fenster et al., 1973) was employed with a unity gain summing amplifier built into the PMT housing. The amplifier was of local design. The transient signal was recorded with a Biomation 8100 transient digitizer interfaced to an IBM-XT at a resolution of 10 ns per point. The excitation response curve $E(t)$ for the laser and detection system was recorded under the same conditions by using light scattered from a buffer solution with the optical filters removed. The experimental transient was then fit by the convolution function $D(t) = \sum E(t_j)i(t-t_j)$, where $i(t)$ is the theoretical response of the system to an infinitely sharp laser pulse

Scheme I



(Demas, 1983). The transients of the three species shown in Scheme I could be detected by the proper choice of wavelengths. The transient at 556.5 nm was assigned to Ru^{II*} , since this is an isobestic point for cytochrome *c*. The $i(t)$ value for this species is

$$i(Ru^{II*}, 556) = \Delta\epsilon_{556}C_0e^{-(k_1+k_d)t} \quad (1)$$

where $\Delta\epsilon_{556}$ is the extinction coefficient for Ru^{II*} , C_0 is the concentration of Ru^{II} molecules excited by the laser pulse, and the rate constants are defined in Scheme I. The transient for Ru^{II*} was also obtained from the luminescence transient decay measured as described by Pan et al. (1988) and fit by using

$$i(Ru^{II*}, \text{luminescence}) = I_0e^{-(k_1+k_d)t} \quad (2)$$

The absorption transient at 550 nm contains a major contribution from Fe^{II} and a small contribution from Ru^{II*} . The contribution from Fe^{II} was obtained by subtracting the Ru^{II*} transient measured at 556.5 nm from the transient at 550 nm, taking into account the slight difference in the extinction coefficients for Ru^{II*} at 550 and 556.5 nm (Figure 2). The 550-nm transient due to Fe^{II} was then fit by the convolution function according to

$$i(Fe^{II}, 550) = A[e^{-(k_1+k_d)t} - e^{-k_2t}] \quad (3)$$

where $A = k_1\Delta\epsilon_{550}C_0/(k_2 - k_1 - k_d)$ and $\Delta\epsilon_{550} = 18.6 \text{ mM}^{-1}$ is the extinction coefficient for the heme. The absorption transient at 440 nm is dominated by the recovery of Ru^{II} following a laser pulse. The small contribution due to heme Fe^{II} was determined from the transient at 550 nm and subtracted by using appropriate extinction coefficients. The 440-nm transient due to Ru^{II} was then fit by the convolution function according to

$$i(Ru^{II}, 440) = \Delta\epsilon_{440}C_0[1 - Be^{-(k_1+k_d)t} + Ce^{-k_2t}] \quad (4)$$

where $B = (k_2 - k_d)/(k_2 - k_1 - k_d)$, $C = k_1/(k_2 - k_1 - k_d)$, and $\Delta\epsilon_{440} = 12 \text{ mM}^{-1}$ (Lachish et al., 1979). The values of k_1 , k_2 , and k_d were systematically varied to simultaneously optimize the fits to all of the above transients, taking into account the relative amplitudes as well as the time dependencies. For each of the derivatives studied, a unique set of values for k_1 , k_2 , and k_d was necessary in order to simultaneously fit all of the transients. Since the transients represented by eq 1, 3, and 4 have completely different functional forms, the calculated rate constants were overdetermined by the experimental data. The unique fits obtained support the mechanism shown in Scheme I.

RESULTS

Preparation of $Ru(bpy)_2(dcbpy)$ -Cytochrome *c* Derivatives. Modification of cytochrome *c* lysine amino groups with the

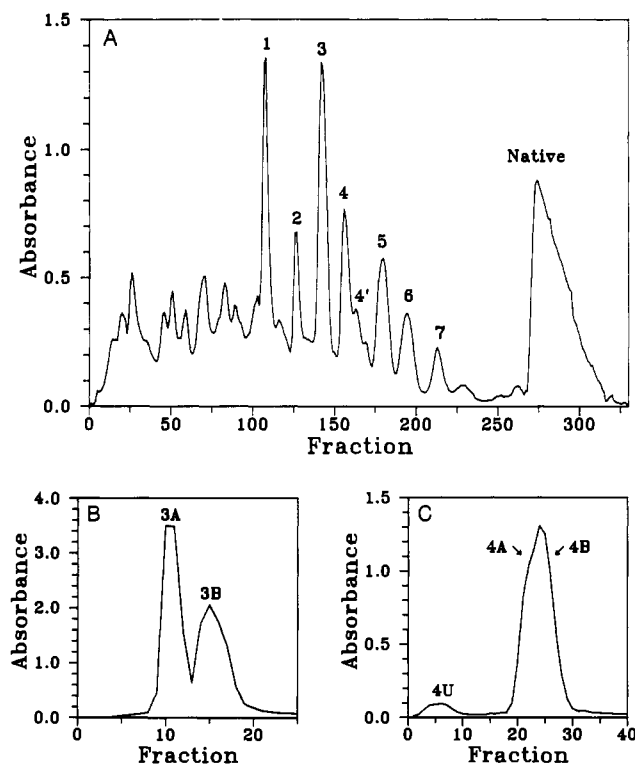


FIGURE 1: Purification of $\text{Ru}(\text{bpy})_2(\text{dcbpy})$ -cytochrome *c* derivatives. (A) The crude reaction mixture of dcbpy-cytochrome *c* (500 mg) was chromatographed on a 2.5×70 cm Bio-Rex 70 column using an exponential gradient from 50 mM ammonium phosphate, pH 7.2, to 160 mM ammonium phosphate, pH 7.2. The flow rate was 25 mL/h, and the fraction size was 3.8 mL. The absorbance was measured at 542 nm. (B) Fraction 3 from A was rechromatographed on a 1.5×25 cm column of Whatman sulfopropyl SE-53 using an exponential gradient from 20 to 250 mM sodium phosphate, pH 6.0. The fraction size was 1 mL, and the absorbance was measured at 542 nm. (C) Repurified fraction 4 was treated with $\text{Ru}^{\text{II}}(\text{bpy})_2(\text{CO}_3)$ and chromatographed on a 0.6×45 cm Whatman CM-32 column using a gradient from 20 to 400 mM sodium phosphate, pH 6.0. The fraction size was 1 mL, and the absorbance was measured at 542 nm. The fraction marked 4U contained unmodified dcbpy-cytochrome *c*.

N-hydroxysuccinimide ester of dcbpy and separation of the dcbpy-cytochrome *c* derivatives on a Bio-Rex 70 column was carried out as described by Pan et al. (1988), except that fraction 4 was resolved into two separate fractions, 4 and 4' (Figure 1A). Fractions 1-3 were resolved into subfractions by rechromatography on a Whatman SE-53 column (Figure 1A), while fractions 4-7 were not further resolved. Each of the purified dcbpy-cytochrome *c* fractions was then incubated with $\text{Ru}^{\text{II}}(\text{bpy})_2(\text{CO}_3)$ at pH 4 to form $\text{Ru}^{\text{II}}(\text{bpy})_2(\text{dcbpy})$ -cytochrome *c* derivatives and purified a final time on a Whatman CM-52 column (Figure 1C). Fractions from the leading and trailing edges of the final chromatograms of fractions 4A and 5 were analyzed separately. HPLC peptide mapping indicated that fractions 3B, 4A, 4B, and 4' were singly modified at lysines 8, 25, 27, and 7, respectively. Fraction 6 was found to contain a 50:50 mixture of derivatives modified at lysines 99 and 100. The other derivatives shown in Table I were previously identified by Pan et al. (1988). The 695-nm band was unmodified in all of the derivatives, indicating that the Met 80 heme ligand remained intact. Heme group redox potentials of the derivatives were all in the range 250-260 mV, essentially the same as that of native cytochrome *c*, 260 ± 10 mV.

Photoinduced Transient Absorption Kinetics. Pan et al. (1988) previously observed that luminescence decay rates of the derivatives were inversely related to the distances between

Table I: Electron-Transfer Rate Constants of $\text{Ru}^{\text{II}}(\text{bpy})_2(\text{dcbpy})$ -Cytochrome *c* Derivatives^a

fraction	lysine modified	k_1	k_2	k_d^b	distance (Å)
1A	86			4.3 ± 0.2	9-20
1B	87			3.5 ± 0.2	10-22
2B	13	16 ± 3	26 ± 5	8 ± 3	6-10
3A	72	14 ± 3	24 ± 5	6 ± 3	8-16
3B	8			5.0 ± 0.5	14-19
4A	25	1.0 ± 0.3	1.5 ± 0.3	6 ± 1	9-16
4B	27	20 ± 3	30 ± 5	20 ± 7	6-12
4'	7	0.3 ± 0.1	0.6 ± 0.2	2.0 ± 0.3	9-16
5A	39 (64%)			4.3 ± 0.2	12-15
	60 (36%)				13-16
6	99 (50%)			3.3 ± 0.3	13-16
	100 (50%)				13-16

^a The absorbance and luminescence transients were measured for each derivative in 100 mM sodium phosphate, pH 7.0, at 25 °C as described in Figures 3-6 and fitted by convolution functions as described under Experimental Procedures. All of the rate constants are in units of 10^6 s^{-1} . ^b The k_d values for the derivatives that did not have a measurable electron-transfer transient was taken to be equal to the luminescence decay rate.

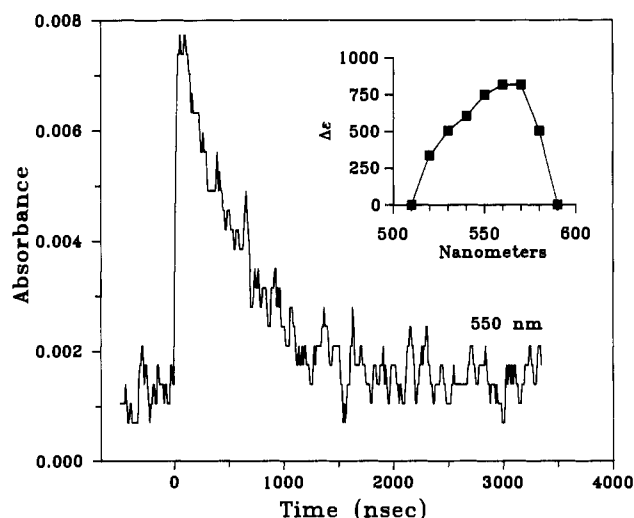


FIGURE 2: Absorption transient of $\text{Ru}^{\text{II}}(\text{bpy})_3$ (20 μM in 100 mM phosphate, pH 7.0) recorded at 550 nm following a 25-ns laser pulse at 460 nm. Inset: The amplitude of the transient was measured as a function of wavelength and plotted as the difference in extinction coefficients of $\text{Ru}^{\text{II}*}$ and Ru^{II} . The difference extinction coefficients at the various wavelengths were calculated by assuming a difference extinction coefficient of -12000 M^{-1} at 440 nm (Lachish et al., 1979).

the Ru^{II} group and the heme group. This observation is consistent with the electron-transfer quenching mechanism suggested by Sutin and Creutz (1978) (Scheme I). However, since an energy-transfer quenching mechanism is also possible, a direct transient absorbance kinetic study was initiated. During the course of this work it was discovered that photoexcitation of $\text{Ru}^{\text{II}}(\text{bpy})_3$ resulted in a weak positive absorption transient in the 520-590-nm range in addition to the well-known negative absorption transient centered at 450 nm (Figure 2). This transient was assigned to $\text{Ru}^{\text{II}*}(\text{bpy})_3$ since $\text{Ru}^{\text{II}}(\text{bpy})_3$ does not absorb at this wavelength, and since the lifetime of the transient was identical with that of the luminescence of $\text{Ru}^{\text{II}*}(\text{bpy})_3$. Photoexcitation of $\text{Ru}(\text{bpy})_2(\text{dcbpy})$ -cytochrome *c* derivatives modified at lysines 8, 39, 60, 86, 87, 99, and 100 resulted in a transient with the same wavelength dependence as that shown in Figure 2, with no evidence for an additional transient at 550 nm associated with electron transfer to the heme group. It was estimated that rate constants k_1 and k_2 for electron transfer in these derivatives must be less than 10^5 s^{-1} . This lower limit in the rate

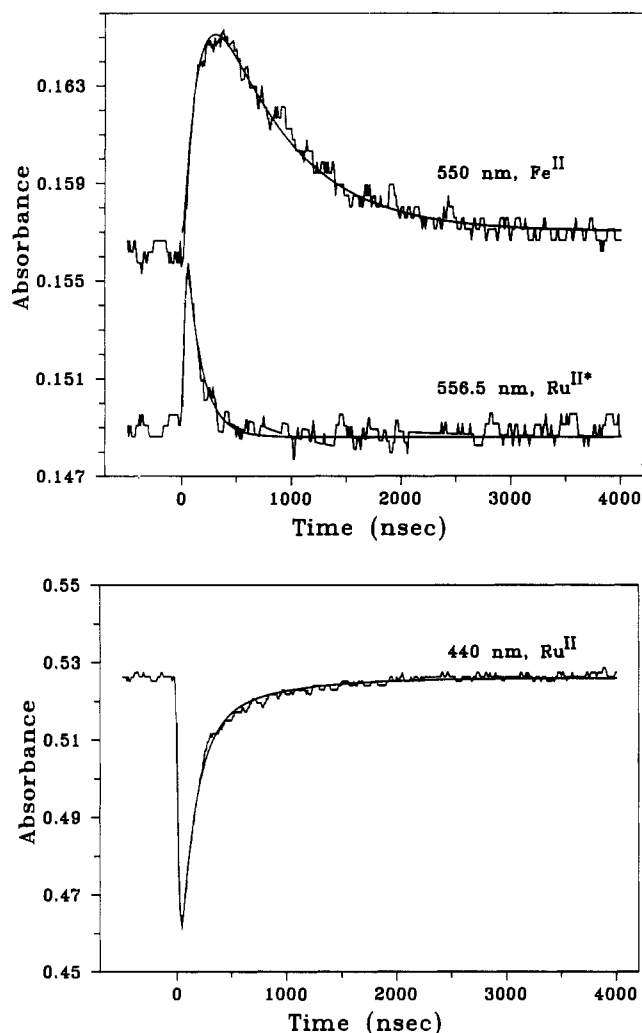


FIGURE 3: Absorption transient of $\text{Ru}(\text{bpy})_3(\text{dcbpy})\text{-Lys 25 cytochrome } c$ ($20 \mu\text{M}$ in 0.1 M phosphate, $\text{pH } 7.0$) following a 25-ns laser pulse at 460 nm . (Top) The transient recorded at 556.5 nm was assigned to $\text{Ru}^{\text{II}*}$. The transient labeled " $550 \text{ nm}, \text{Fe}^{\text{II}}$ " was obtained from the difference between the 550- and 556.5-nm transients as described under Experimental Procedures and was due to the formation and decay of Fe^{II} . (Bottom) The transient at 440 nm was due to the recovery of Ru^{II} following the laser pulse. Each transient shown is the average of 10 individual transients. Transients at different wavelengths were obtained under identical conditions. The smooth lines give the optimized fits of the appropriate convolution functions to the experimental transients.

constant window available in the present experiments is determined by the signal to noise ratio and the value of k_d .

The remaining derivatives all exhibited transients associated with electron transfer, and it was possible to follow the time course of each of the species shown in Scheme I. Figure 3 shows the transients for the derivative modified at lysine 25, which is $9\text{--}16 \text{ \AA}$ from the heme group. The transient at 556.5 nm was assigned to $\text{Ru}^{\text{II}*}$, since this is an isobestic point for the heme group. The rate constant for this transient, $7 \times 10^6 \text{ s}^{-1}$, was identical with that of the luminescence transient and fixes the value of $k_1 + k_d$. The Fe^{II} transient was obtained by subtracting the $\text{Ru}^{\text{II}*}$ transient measured at 556.5 nm from the 550-nm transient, taking into account the slight difference in the extinction coefficients of $\text{Ru}^{\text{II}*}$ at the two wavelengths. The rise and fall times of the resulting Fe^{II} transient were much slower than those of the 556.5-nm transient, consistent with an electron-transfer process. The 440-nm transient was due to the recovery of Ru^{II} following a laser pulse. The wavelength dependence of this transient was nearly identical with that of $\text{Ru}^{\text{II}}(\text{bpy})_3$ (Lachish et al., 1979), and the transient was present

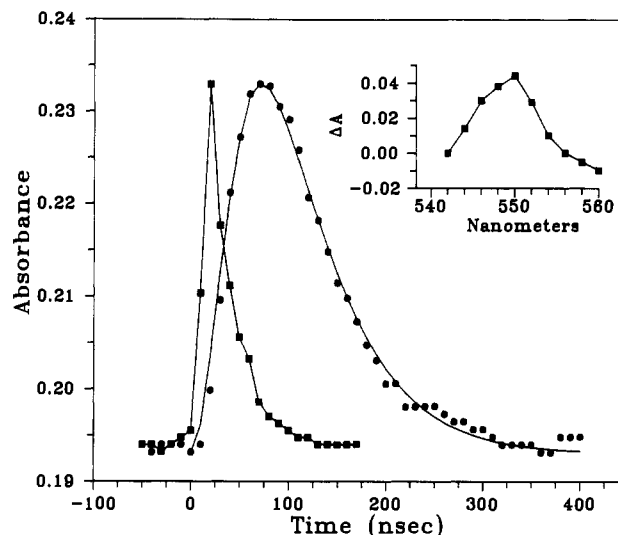


FIGURE 4: Absorption transient of $\text{Ru}(\text{bpy})_3(\text{dcbpy})\text{-Lys 72 cytochrome } c$ ($20 \mu\text{M}$) at 550 nm following a 25-ns laser pulse at 460 nm . The excitation response $E(t)$ of the detection system is given by (■), while the 550-nm transient of the derivative is given by (●). The inset shows the wavelength dependence of the amplitude of the transient. The experimental conditions are the same as those given in Figure 3.

at 434 nm , which is an isobestic point for the heme group. All transients were corrected and fitted to appropriate convolution functions as described under Experimental Procedures. A unique set of values for k_1 , k_2 , and k_d was necessary in order to simultaneously fit all of the transients. These values were $k_1 = 1 \pm 0.3$, $k_2 = 1.5 \pm 0.3$, and $k_d = 6 \pm 1$, all in units of 10^6 s^{-1} . The amplitude of the 550-nm transient was relatively small compared to the 440-nm transient because k_d was large compared to k_1 , and other quenching mechanisms decreased the relative extent of electron transfer. Rate constants obtained from absorbance transients were independent of concentration over the range investigated ($5\text{--}20 \mu\text{M}$), while rate constants for the luminescence transients were independent of concentration from 0.5 to $20 \mu\text{M}$.

Derivatives modified at lysines 13, 27, and 72 near the heme crevice had very large rate constants ranging from 14×10^6 to $30 \times 10^6 \text{ s}^{-1}$. Figure 4 shows that the 550-nm transient for the lysine 72 derivative had a much larger amplitude than that of the lysine 25 derivative, as well as much faster rise and fall times. The wavelength dependence of this transient was nearly identical with the difference spectrum of the heme group (inset, Figure 4), and the contribution from $\text{Ru}^{\text{II}*}$ was less than 15%. Optimized values of the rate constants were $k_1 = 14 \pm 3$, $k_2 = 24 \pm 3$, and $k_d = 6 \pm 3$ in units of 10^6 s^{-1} . Similar results were obtained for derivatives modified at lysines 13 and 27 (Figure 5 and Table I). Since the lifetimes of these transients were somewhat close to the response time of the digitizer, experiments were also carried out by using a storage oscilloscope with a faster response time. Essentially the same results were obtained, validating the convolution process used (Demas, 1983). The lysine 7 derivative also had a detectable Fe^{II} transient at 550 nm , but its amplitude was very small compared to that of the 440-nm transient, and the electron-transfer rate constants were even slower than those of the lysine 25 derivative (Figure 6 and Table I). These rate constants probably represent the lower limit of electron-transfer rates that can be measured with the current method.

DISCUSSION

The $\text{Ru}^{\text{II}}(\text{bpy})_3(\text{dcbpy})\text{-lysine}$ complex has a number of favorable properties for the study of biological electron-transfer

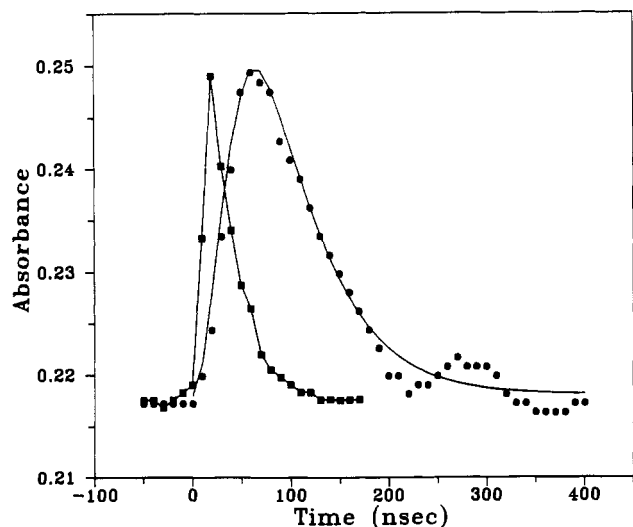


FIGURE 5: Absorption transient of Ru(bpy)₂(dcbpy)-Lys 27 cytochrome *c* (20 μM) at 550 nm following a 25-ns laser pulse at 460 nm. The conditions are the same as those given in Figure 3.

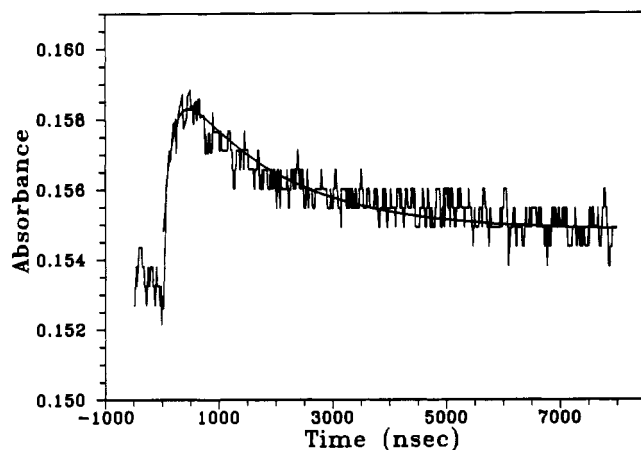


FIGURE 6: Absorption transient of Ru(bpy)₂(dcbpy)-Lys 7 cytochrome *c* (20 μM) at 550 nm following a 25-ns laser pulse at 460 nm. The conditions are the same as those given in Figure 3.

reactions. It can be photoexcited to a metal-to-ligand charge-transfer excited state, Ru^{II*}, that is equivalent to that of the well-known Ru(bpy)₃ complex (Cherry & Henderson, 1984). This state has a natural lifetime of about 600 ns and is both a strong oxidizing agent and a strong reducing agent. Electron-transfer reactions of Ru^{II*}(bpy)₃ and Ru^{III}(bpy)₃ are characterized by high driving forces and low reorganization barriers (Sutin, 1982). Therefore, Ru(bpy)₂(dcbpy)-cytochrome *c* derivatives provide an opportunity to study electron-transfer properties of the native heme group iron at high driving force with a minimum contribution to the reorganization energy from the ruthenium complex. These derivatives have the same heme redox potentials and spectral properties as native cytochrome *c* and retain high enzymatic activity with cytochrome oxidase (Pan et al., unpublished observation). Previous studies at high driving forces have involved substituting native iron with zinc, which of course alters the redox properties of the cytochrome and destroys enzymatic activity (Elias et al., 1988). Excited- and ground-state properties of the Ru(bpy)₂(dcbpy) complex attached to cytochrome *c* are essentially identical with those of the free deprotonated complex. Both have luminescence maxima of 662 nm at 298 K which shift to 606 nm at 77 K. The luminescence decay rate constant k_d of a derivative made from lysozyme, a protein with no heme iron, is $1.8 \times 10^6 \text{ s}^{-1}$, which is nearly identical with

that of Ru^{II*}(bpy)₂(dcbpy) and Ru^{II*}(bpy)₃ (Cherry & Henderson, 1984; Pan et al., 1988).

Photoinduced electron-transfer kinetics of all of the Ru(bpy)₂(dcbpy)-cytochrome *c* derivatives were found to be consistent with Scheme I. The rate constant k_d includes all processes that do not involve electron transfer, including radiative and nonradiative quenching as well as energy-transfer quenching. All of the derivatives had larger k_d values than that of Ru(bpy)₂(dcbpy)-lysozyme (Table I). This underlines the need for complete kinetic studies of the absorption transients of each species in order to distinguish between electron-transfer and energy-transfer quenching mechanisms.

Electron-transfer rate constants k_1 and k_2 for the derivatives modified at lysines 13, 27, and 72 surrounding the heme crevice are the largest first-order rate constants ever detected for a native heme group in a cytochrome, ranging from 14×10^6 to $30 \times 10^6 \text{ s}^{-1}$. Significantly smaller rate constants were observed for derivatives modified at lysines further removed from the heme group, down to less than 10^5 s^{-1} . It is informative to compare the observed rate constants with those predicted by the widely used semiclassical treatment introduced by Marcus (Marcus, 1965; Marcus & Sutin, 1985):

$$k_{et} = 10^{13} \exp[-\beta(d-3)] \exp[-(\lambda + \Delta G^\circ)^2/4\lambda RT] \quad (5)$$

In this expression λ is the vertical reorganization energy, ΔG° is the reaction free energy, β is a scalar describing how rapidly the rate decreases with increasing separation distance, and d is the distance between the donor and acceptor atoms. The ΔG° values for the forward and reverse electron-transfer reactions have been estimated to be 0.98 and 1.05 V, respectively, based on $E^\circ(\text{II}^*/\text{III}) = -0.72 \text{ V}$ and $E^\circ(\text{II}/\text{III}) = 1.31 \text{ V}$ for Ru(bpy)₂(dcbpy) and $E^\circ = 0.26 \text{ V}$ for cytochrome *c*. Values for β are somewhat variable, but $0.9\text{--}1.2 \text{ \AA}^{-1}$ appears to be representative (Axup et al., 1988; Elias et al., 1988). Studies of Ru^{II}(bpy)₃ self-exchange suggest that the distance is best measured from the ligand atoms because of the delocalization of metal electron density onto the bipyridines. A similar assumption was used by Axup et al. (1988) in their analysis of electron transfer in Ru(NH₃)₅(his) myoglobin. The distances given in Table I were estimated by using a model of the X-ray crystal structure of cytochrome *c* (Swanson et al., 1977) with a space-filling model of the ruthenium complex attached to the appropriate lysine. The distance was measured between a ruthenium bipyridine ring atom and the iron ligand atom that was closest to it (either a porphyrin ring atom, a histidine 18 ring atom, or the methionine 80 sulfur atom). All possible orientations of the lysine side chain that did not bring any atoms closer than van der Waals contact were taken into account to estimate the extreme limits of the possible distances. All of the lysine residues are on the surface of the protein and are fully accessible to solvent.

By use of the parameters described above, eq 5 was used to predict the distance dependence of rate constant k_2 for reaction of Ru^{III}(bpy)₂(dcbpy) with heme Fe^{II} (Figures 7 and 8). Despite relatively large uncertainties in distances, limits could be placed on the reorganization energy from a comparison of rate constants of different derivatives. If β was assumed to be 0.9 \AA^{-1} , two different solutions for the reorganization energy were possible, $\lambda = 0.44 \pm 0.03 \text{ eV}$ and $\lambda = 2.4 \pm 0.1 \text{ eV}$. Assuming $\beta = 1.2 \text{ \AA}^{-1}$, the two solutions were $\lambda = 0.50 \pm 0.05$ and $2.1 \pm 0.1 \text{ eV}$. Individual reorganization energies for cytochrome *c* and Ru^{II}(bpy)₃ have been estimated from self-exchange data to be 1.0 and 0.57 eV, respectively (Marcus & Sutin, 1985; Brown & Sutin, 1979). On the basis of these values, the reorganization energy for electron transfer in Ru(bpy)₂(dcbpy)-cytochrome *c* derivatives would be pre-

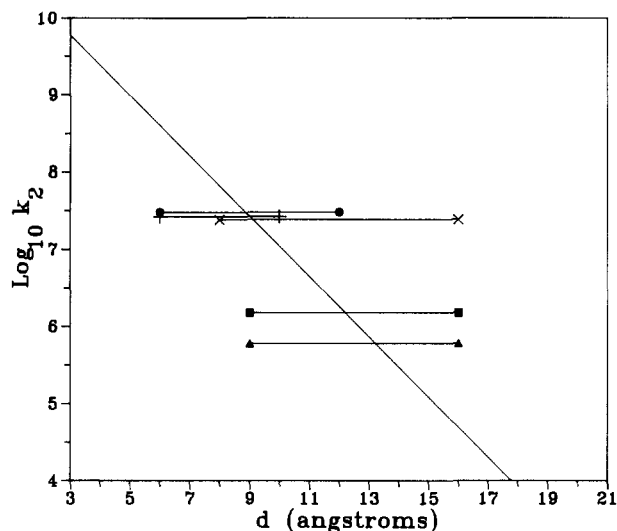


FIGURE 7: Plot of the logarithm of the rate constant versus the separation distance d . Experimental data points are given for derivatives modified at lysines 7 (Δ), 13 ($+$), 25 (\blacksquare), 27 (\bullet), and 72 (\times) at the minimum and maximum estimates of the separation d . The theoretical line (—) is based on eq 5 using $\beta = 0.9 \text{ \AA}^{-1}$ and $\lambda = 0.44$ or 2.4 eV .

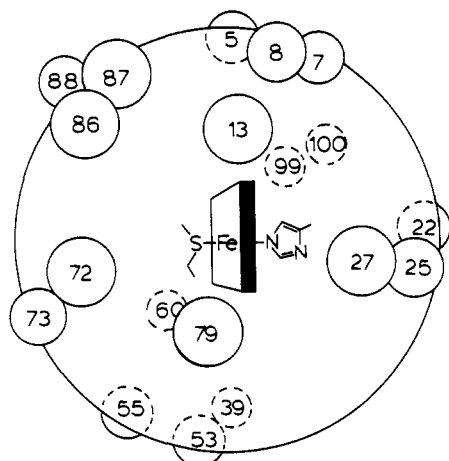


FIGURE 8: Schematic diagram of horse heart cytochrome c viewed from the front of the heme crevice. The approximate positions of the β carbon atoms of the lysine residues are indicated by closed and dashed circles for residues located toward the front and back of cytochrome c , respectively.

dicted to be 0.8 eV , which is closer to the lower of the two values given above. However, Karas et al. (1988) have recently estimated the reorganization energy to be $1.9\text{--}2.45 \text{ eV}$ for electron transfer in metal-substituted myoglobin–ruthenium complexes. Derivatives with separation distances greater than 15 \AA are predicted to have rate constants less than 10^5 s^{-1} by the above treatment. This is consistent with the absence of any detectable electron-transfer transient for derivatives modified at lysines farther than 15 \AA from the heme group.

It is significant that the ratio of the forward to reverse rate constants was about $1:1.5$ for all derivatives. This near-unity ratio is consistent with the nearly identical driving forces for the forward and reverse reactions. It also indicates that there were no conformational changes that would discriminate between the forward and reverse reactions for any of the derivatives. Bechtold et al. (1986) have invoked such "directional" conformational changes to rationalize the very slow rate of the $\text{Ru}^{\text{III}}(\text{NH}_3)_4(\text{isonicotinamide})\text{--His 33}$ cytochrome c derivative compared to the rate of the $\text{Ru}^{\text{II}}(\text{NH}_3)_5\text{--His 33}$ cytochrome c derivative. Jackman et al. (1988) have also discussed the importance of intervening

protein structure to electron transfer in connection with their studies of two algal plastocyanins labeled with $\text{Ru}(\text{NH}_3)_5$ at histidine 59 (Jackman et al., 1988). The rate of electron transfer between the ruthenium complex and the copper was less than 0.082 s^{-1} , even though the distance was about the same as that in the cytochrome c derivative ($10\text{--}12 \text{ \AA}$), and the driving force was favorable.

We are currently exploring the use of sacrificial redox agents that react with one of the redox states of ruthenium and alter the electron-transfer pathway shown in Scheme I. For example, all of the derivatives are rapidly photoreduced by EDTA, which reacts with Ru^{III} to form Ru^{II} and prevent the back-reaction (Pan et al., unpublished observations). This rapid photoreduction occurs even in those derivatives labeled on the back side of cytochrome c that do not have a detectable 550-nm transient in the absence of EDTA. This observation indicates that electron transfer occurs in these derivatives, but at a rate less than 10^5 s^{-1} . We have recently prepared two new cytochrome c derivatives labeled with $\text{Ru}^{\text{II}}(\text{bpy})_2(\text{imidazole})$ at histidines 26 and 33, respectively (Durham et al., 1989). These derivatives have a luminescent excited state that might be useful in photoinduced electron-transfer studies.

REFERENCES

- Anderson, G. W., Zimmerman, J. E., & Callahan, F. M. (1964) *J. Am. Chem. Soc.* **86**, 1839–1842.
- Axup, A. W., Albin, M., Mayo, S. L., Crutchley, R. J., & Gray, H. B. (1988) *J. Am. Chem. Soc.* **110**, 435–439.
- Bechtold, R., Kuehn, C. L., & Isied, S. S. (1986) *Nature* **322**, 286–289.
- Cherry, W. R., & Henderson, L. J., Jr. (1984) *Inorg. Chem.* **23**, 983–986.
- Closs, G. L., Calcaterra, L. T., Green, N. J., Penfield, K. W., & Miller, J. R. (1986) *J. Phys. Chem.* **90**, 3673–3683.
- Crutchley, R. J., Ellis, W. R., Jr., & Gray, H. B. (1986) *Frontiers in Bioinorganic Chemistry* (Xavier, A. V., Ed.) VCH, Weinheim, FRG.
- Demas, J. N. (1983) *Excited State Lifetime Measurements*, Academic Press, New York.
- Durham, B., Pan, L. P., Hahm, S., Hall, J., & Millett, F. (1989) *Inorganic Symposium on Biological Electron Transfer*, ACS Advances in Chemistry Series, (submitted for publication).
- Elias, H., Chou, M. H., & Winkler, J. R. (1988) *J. Am. Chem. Soc.* **110**, 429–434.
- Elliott, C. M., & Hershenhart, E. J. (1982) *J. Am. Chem. Soc.* **104**, 7519–7526.
- Fenster, A., LeBlanc, J. C., Taylor, W. B., Johns, H. E. (1973) *Rev. Sci. Instrum.* **44**, 689–694.
- Isied, S. S., Worosila, G., & Atherton, S. J. (1982) *J. Am. Chem. Soc.* **104**, 7659–7661.
- Jackman, M. P., McGinnis, J., Powls, R., Salmon, G. A., & Sykes, A. G. (1988) *J. Am. Chem. Soc.* **110**, 5880–5887.
- Johnson, E. C., Sullivan, B. P., Salmon, D. J., Adege, S. A., & Meyer, T. J. (1978) *Inorg. Chem.* **17**, 2211–2215.
- Kostić, N. M., Margalit, R., Che, C.-M., & Gray, H. B. (1983) *J. Am. Chem. Soc.* **105**, 7765–7767.
- Lachish, U., Infelta, P. P., & Gratzel, M. (1979) *Chem. Phys. Lett.* **62**, 317–319.
- Marcus, R. A. (1965) *J. Chem. Phys.* **43**, 679–701.
- Marcus, R. A., & Sutin, N. (1985) *Biochim. Biophys. Acta* **811**, 265–322.
- McGourty, J. L., Peterson-Kennedy, S. E., Ru, W. Y., & Hoffman, B. M. (1987) *Biochemistry* **26**, 8302–8312.
- Nocera, D. G., Winkler, J. R., Yocom, K. M., Bordignon, E., & Gray, H. B. (1984) *J. Am. Chem. Soc.* **106**, 5145–5150.

- Pan, L. P., Durham, B., Wolinska, J., & Millett, F. S. (1988) *Biochemistry* 27, 7180-7184.
 Smith, H. T., Staudenmeyer, N., & Millett, F. (1977) *Biochemistry* 16, 4971-4975.
 Sprintschnik, G. H. W., Dirsch, P. P., & Whitten, D. G. (1977) *J. Am. Chem. Soc.* 99, 4947.

- Sutin, N. (1982) *Acc. Chem. Res.* 15, 275-282.
 Sutin, N., & Creutz, C. (1978) *Adv. Chem. Ser.* 168, 1-27.
 Swanson, T., Trus, B. L., Mandel, N., Mandel, G., Kallai, O., & Dickerson, R. E. (1977) *J. Biol. Chem.* 252, 759-770.
 Winkler, J. R., Nocera, D. G., Yocom, K. B., Bordignon, E., & Gray, H. B. (1982) *J. Am. Chem. Soc.* 104, 5798-5800.

Complete Primary Structure of a *Lolium perenne* (Perennial Rye Grass) Pollen Allergen, *Lol p* III: Comparison with Known *Lol p* I and II Sequences[†]

Aftab A. Ansari,*[‡] Ponniah Shenbagamurthi,[§] and David G. Marsh[‡]

Clinical Immunology Division, Department of Medicine, The Johns Hopkins University School of Medicine, 5601 Loch Raven Boulevard, Baltimore, Maryland 21239, and Department of Biological Chemistry, The Johns Hopkins University School of Medicine, Baltimore, Maryland 21205

Received May 2, 1989; Revised Manuscript Received June 27, 1989

ABSTRACT: The complete amino acid sequence of a *Lolium perenne* (rye grass) pollen allergen, *Lol p* III, determined by the automated Edman degradation of the protein and its selected fragments, is reported in this paper. Cleavage by enzymatic and chemical techniques established unambiguously the sequence for this 97-residue protein ($M_r = 10\,909$), which lacks cysteine and shows no evidence of glycosylation. The sequence of *Lol p* III is very similar to that of another *L. perenne* allergen, *Lol p* II, which was sequenced recently; of the 97 positions in the two proteins, 57 are occupied by identical amino acids (59% identity). In addition, both allergens share a similar structure with an antibody-binding fragment of a third *L. perenne* allergen, *Lol p* I. Since human antibody responsiveness to all these three allergens is associated with HLA-DR3, and since the structure common to the three molecules shows high degrees of amphipathicity in *Lol p* II and III, we speculate that this common segment in the three molecules might contain or contribute to the respectively Ia/T-cell sites.

Protein antigens contain two classes of epitopes: B-cell epitopes, which are recognized by specific antibodies, and Ia/T-cell epitopes, which are recognized by an MHC¹ (Ia) molecule and a T-cell receptor. In vivo, the antigen molecule is cleaved into smaller fragments inside an antigen presenting cell (APC), such as a macrophage, a dendritic cell, a B cell, etc.; one or more fragments containing Ia/T-cell epitope(s) bind to an Ia molecule, and this antigen-Ia complex is presented by the APC to a specific T-cell receptor on a helper T cell (Schwartz, 1985). The T cell is stimulated to proliferate clonally and secrete interleukins, which activate B cells to proliferate clonally, differentiate, and produce antibodies specific for the B-cell epitopes of the antigen. An understanding of the genetic control of the human immune response requires delineating the structures (Ia/T-cell sites) in an antigen molecule that are presented to the T cells by Ia molecules. We have been studying the genetics of human immune responsiveness using the *Lolium perenne* (rye grass) pollen allergens *Lol p* I, II, and III as model antigens.

Lol p I (Rye I), the major allergen of *L. perenne* pollen, is a glycoprotein ($M_r = 27\,000$ – $32\,000$) toward which 85–90% of grass-allergic patients are sensitive (Freidhoff et al., 1986); *Lol p* II and III are proteins ($M_r = 11\,000$ in both cases) toward which 45% of grass-allergic patients are sensitive in each case (Freidhoff et al., 1986; Ansari et al., unpublished observation). Immunologically, *Lol p* II and III are cross-reactive with each other, but neither shows any cross-reactivity with *Lol p* I (Ansari et al., 1987). All of these allergens exist in multiple "isoallergenic" forms which are variants but appear to be immunologically indistinguishable (Johnson & Marsh, 1965a,b). *Lol p* III is a group of basic proteins with isoelectric points in the range of 9.0–9.4, with the main isoallergenic forms *Lol p* IIIB ($pI = 9.0$) and *Lol p* IIIA ($pI = 9.4$), the former being the more abundant quantitatively.

The *Lol p* allergens have proved important in studies concerning the genetics of human immune responsiveness (Freidhoff et al., 1988; Ansari et al., 1989a,b). We have found that human IgE and IgG Ab responsiveness to *Lol p* I–III is significantly associated with HLA-DR3; in the case of *Lol p* III the association extends to DR5 also. The partial sequence

[†] This work was supported by Grants AI-19727 and AI-25372 from the National Institutes of Health and by Johns Hopkins Institutional Grant M-53-1007. This is Publication No. 764 from the O'Neill Laboratories, The Good Samaritan Hospital, Baltimore, MD.

* Address correspondence to this author at the Clinical Immunology Division, Department of Medicine, The Johns Hopkins University School of Medicine, 5601 Loch Raven Blvd., Baltimore, MD 21239.

[‡] Department of Medicine, The Johns Hopkins University School of Medicine.

[§] Department of Biological Chemistry, The Johns Hopkins University School of Medicine.

¹ Abbreviations: Ab, antibody; HLA, human leucocyte antigen; HPLC, high-performance liquid chromatography; rpHPLC, reverse-phase HPLC; *Lol p* I, II, and III, designations given under the IUIS Allergen Nomenclature System (Marsh et al., 1986) for *Lolium perenne* pollen allergens previously known as Rye I, II, and III, respectively; MHC, major histocompatibility complex; RIA, radioimmunoassay; TFA, trifluoroacetic acid; TPCK, tosylphenylalanine chloromethyl ketone; TLCK, tosyllysine chloromethyl ketone.